Chapter 4 Tires, Wheels, and Brakes

4.1. Introduction

The number of tires required for a given aircraft design gross weight is largely determined by the flotation characteristics, which will be discussed in detail in Chapter Seven. Assuming that the number and distribution pattern of the tires is already known, this chapter provides guidelines to the selection of the tires, wheels, and brakes that will meet the performance and safety requirements [2 and 20].

As a part of the landing gear configuration definition process, tires, wheels, and brakes selection algorithms were developed based on the procedure as discussed in this chapter. Specified selection criterion, *e.g.*, minimum size, weight, or pressure, are used to select suitable tires and wheels from manufacturer's catalog [24] and industry standards [25], while statistical database was used to size the brakes as required to meet the braking requirements.

4.2. Type, Size and Inflation Pressure of the Tire

The tire selection process involves listing all candidates that meet the performance requirements. A list of tires and wheels used on commercial transports can be found in Appendix D. The primary consideration is the load-carrying capacity of the tire during the speed regime normally applicable for landing or takeoff cycles. In addition, the number of plys and type of construction, which determines the weight of the tire and its operational life, is important from an economic standpoint. Other considerations include the inflation pressure of the tire and the size of the wheel. The former must be chosen in accordance with the bearing capacity of the airfield from which the aircraft is designed to operate from, whereas the latter must have sufficient space to house the brake assembly.

4.2.1. Basic Tire Constructions

Radial tires have gained growing acceptance since their introduction despite a somewhat cautious approach at the beginning, which is attributed to lack of applicable standards, concerns about the *mixability* with bias tires, and *retreadability* of refurbished tires. Intermixing of radial and bias tires, or even with radial tires of different construction, is possible only if the loading is no more uneven than currently encountered with mixing of bias tires only. As for retreadability, it should be noted that multiple retreating is not necessarily a benefit to the airlines; instead, it could be an indication of low tire performance in terms of tread wear. Thus, the concern here is not as much how often the tire can be retreated, but how to extend the average total carcass life.

In radial construction, shear stresses in the rubber matrix are minimized and loads are efficiently distributed throughout the tire. Even if the same basic materials used in bias tires are used in the radials, the amount of material required for a particular application can be reduced. As a result, weight savings of up to 20 percent have been realized [26]. In addition, minimized slippage between the tire and the contact surface and the near optimal tuning of belt stiffness that comes with the radial construction all contributed to improved wear performance. In fact, some radial tires currently achieve twice as many landings per tread as conventional bias tires [26].

Operational experience has also shown that radial tires offer a greater overload bearing capacity and withstand under-inflation better. An approximately 10-percent increase in the footprint area improves the flotation characteristics and reduces hydroplaning on wet runways [26]. In addition, radial tires do not fail as suddenly as bias tires do. Warning signs such as external deformation and out-of-roundness exhibited prior to catastrophic failure provide indications of a potential blowout to maintenance personnel, and thus enhance operational safety.

4.2.2. Size of the Tire

The choice of the main wheel tires is made on the basis of the static loading case. The total main gear load (F_m) is calculated assuming that the aircraft is taxiing at low speed without braking. As shown in Figure 4.1, equilibrium gives [5, p. 356]

$$F_m = \frac{l_n}{l_m + l_n} W \tag{4.1}$$

where W is the weight of the aircraft and l_m and l_n are the distance measured from the aircraft *cg* to the main and nose gear, respectively. The design condition occurs at MTOW with the aircraft *cg* at its aft limit. For single axle configurations, the total load on the strut is divided equally over the tires, whereas in tandem configurations, the load per wheel depends on the location of the pivot point; to reduce overloading of the front wheels during braking, the pivot is usually positioned such that the distance between it and the front and rear wheel axles is about 55 and 45 percent of the truck beam, respectively [5].

The choice of the nose wheel tires is based on the nose wheel load (F_n) during braking at maximum effort, *i.e.*, the steady braked load. Using the symbols shown in Fig. 4.1, the total nose gear load under constant deceleration is calculated using [5, p. 358]

$$F_n = \frac{l_m}{l_m + l_n}(W - L) + \frac{h_{cg}}{l_m + l_n}\left(\frac{a_x}{g} W - D + T\right) \tag{4.2}$$

where L is the lift, D is the drag, T is the thrust, and h_{cg} is the height of aircraft *cg* from the static groundline. Typical values for a_x/g on dry concrete vary from 0.35 for a simple brake system to 0.45 for an automatic brake pressure control system [5]. As both D and L are positive, the maximum nose gear load occurs at low speed. Reverse thrust decreases the nose gear load and hence the condition $T = 0$ results in the maximum value [5, p. 359]

$$F_n = \frac{l_m + h_{cg}(a_x / g)}{l_m + l_n} W \tag{4.3}$$

The design condition occurs at MTOW with the aircraft *cg* at its forward limit.

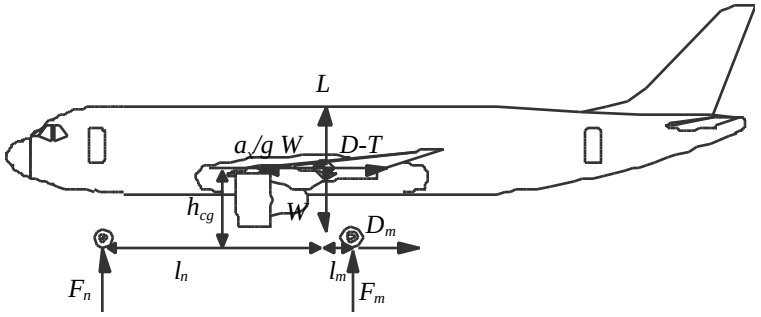

Figure 4.1 Forces acting on the aircraft during a braked roll [5]

To ensure that the rated loads will not be exceeded in the static and braking conditions, a seven percent safety factor is used in the calculation of the applied loads [2]. In addition, to avoid costly redesign as the aircraft weight fluctuates during the design phase, and to accommodate future weight increases due to anticipated aircraft growth, the calculated loads are factored upward by another 25 percent prior to tire selection [2].

4.2.3. Inflation Pressure

Provided that the wheel load and configuration of the landing gear remain unchanged, the weight and volume of the tire will decrease with an increase in inflation pressure. From the flotation standpoint, a decrease in the tire contact area will induce a higher bearing stress on the pavement, thus eliminates certain airports from the aircraft's operational bases. Braking will also become less effective due to a reduction in the frictional force between the tires and the ground. In addition, the decrease in the size of the tire, and hence the size of the wheel, could pose a problem if internal brakes are to be fitted inside the wheel rims. The arguments against higher pressure are of such a nature that commercial operators generally prefer the lower pressures in order to maximize tire life and minimize runway stress [26].

4.3. Wheel Design

The design of the aircraft wheel is influenced primarily by its requirement to accommodate the selected tire, to be large enough to house the brake, and to accomplish the above tasks with minimum weight and maximum life. As shown in Figure 4.2, two basic configurations of wheel design are currently available: A-frame and bowl-type [27]. The former is structurally the most efficient and therefore the lightest that can be achieved. However, this design has a limited space for housing the brake as compared to the bowl-type design. Consequently, as the braking energy requirement increases with aircraft weight and hence the size of the heat sink required, it might be necessary to resort to a bowl-type design even though it has a weight penalty [27].

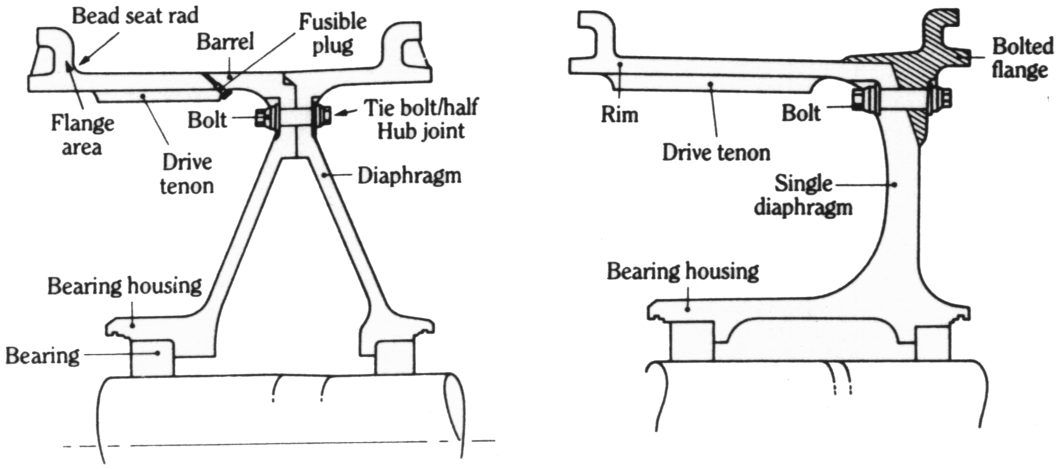

a) A-frame b) Bowl-type

Figure 4.2 Basic configuration of wheel design [27]

Continued heavy dependence on forged aluminum alloy wheels is foreseen by industry, whereas steel and magnesium alloy wheels are no longer given serious consideration due to weight and corrosion problems, respectively [28]. Although practicable, titanium wheels are still quite expensive. Most of the premium for titanium wheels results from the expense for the forging process, which could be 10 to 11 times those of aluminum alloy [28] In addition, current titanium forging tolerances have yet to reach the precision obtainable for aluminum material, thus machining of all surfaces is required to control weight and obtain the desired form.

Based on statistical data, the wheel assembly weight is determined as a function of the rated per wheel static load (F) and average tire outer diameter (D) [2, p. 145]

$$f_w = \frac{FD}{1000} \tag{4.4}$$

Given the type of material to be used, the wheel assembly unit weight is obtained from Figure 4.3 with the weight factor (f_w) as determined from Eq. (4.4).

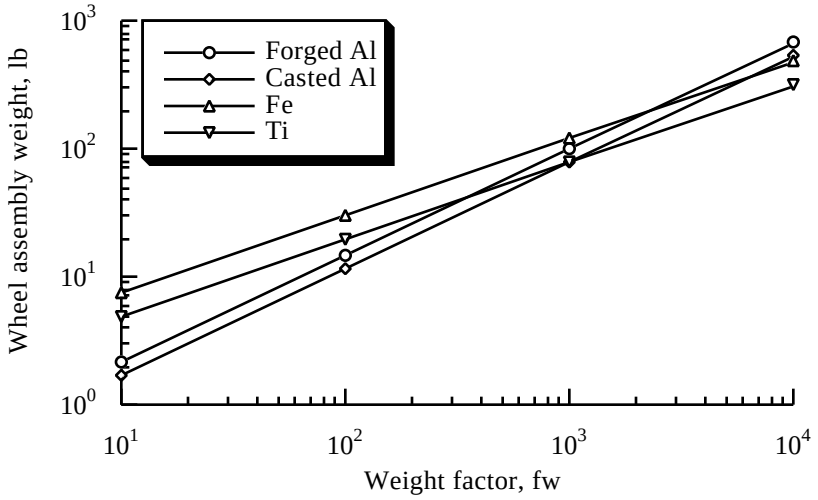

Figure 4.3 Aircraft wheel assembly weight [2]

4.4. Brake Design

Besides the primary task of stopping the aircraft, brakes are used to control speed while taxiing, to steer the aircraft through differential action, and to hold the aircraft stationery when parked and during engine run-up. Since the heat sinks account for a significant fraction of total landing gear weight, there is a continual effort to reduce their weight through the application of advanced materials, namely, carbon [19].

4.4.1. Heat Sink Material

Material characteristics of steel and carbon are compared in Table 4.1. As shown in the table, carbon's high specific heat and thermal conductivity make it highly desirable as a heat absorber. The former ensures a reduction in brake weight, while the latter ensures that the heat transfer throughout the heat sink occurs more uniformly and at a faster rate. In

addition, carbon retains much of its specific strength, which is defined as the ultimate tensile strength divided by density, at high temperature while steel loses almost all of its strength.

Table 4.1 Heat sink materials comparison [2]

Property	Steel	Carbon	Desired
Density, lb/in^3	0.283	0.061	High
Specific heat at 500°F, Btu/lb•°F	0.13	0.31	High
Thermal conductivity at 500°F, Btu/h•ft^2•°F	24.0	100.0	High
Thermal expansion at 500°F, 1.0E-6 in•°F/in	8.4	1.5	Low
Thermal shock resistance index, ×105	5.5	141.0	High
Temperature limit, °F	2,100	4,000	High

Long service life and low maintenance requirements for carbon brakes prove to be another plus from an economic standpoint. It was estimated that carbon would permit up to five to six times more landings as compared to steel between refurbishment and would require fewer man-hours for overhaul [27]. To illustrate the economic advantage of using carbon brakes, it was estimated that a total weight saving of 1,200 pounds could be achieved on the Concorde using carbon brakes. This is equivalent to five percent of its estimated transatlantic payload [29].

The primary drawback of carbon brakes is that a greater volume is required to absorb the same amount of energy in comparison to steel brakes. Some problems with carbon brakes include sudden loss of strength due to oxidation of the carbon, temporary loss of braking due to moisture contamination, and high initial cost. However, these issues have largely been resolved in favor of the performance and economic aspects of carbon heat sinks [16]. In fact, advanced transports such as the Boeing Model 777 and the emerging ultra-high-capacity aircraft all feature carbon brakes.

4.4.2. Brake Sizing

The primary consideration in brake development is the size and weight of the brake required to meet the kinetic energy generated under the design landing weight, maximum landing weight, and rejected takeoff (RTO) conditions. Brake capacity requirements for these braking conditions are listed in Table 4.2.

Table 4.2 FAA commercial transport brake capacity requirements [20]

	Specifications
Design landing weight	100 stops at average of 10 ft/s^2 deceleration
Maximum landing weight	5 stops at average of 10 ft/s^2 deceleration
Rejected takeoff	1 stop at average of 6 ft/s^2 deceleration

The total kinetic energy is determined using the expression [20]

$$KE = 0.0443WV^2 \tag{4.5}$$

where V is the power-off stalling speed in knots. Assuming that the power-off stalling speed is 1.2 times of the stalling speed (V_s), it can be approximated using the expression [5, p. 577]

$$V = 1.2V_S = 1.2\sqrt{\frac{2W}{1.13\rho SC_{L,\max}}} \tag{4.6}$$

where ρ is the standard sea-level air density, S is the reference wing area, and $C_{L,max}$ is the maximum wing lift coefficient. The constant 1.13 takes into account the speed loss in the FAA stall maneuver [5]. As illustrated above, the kinetic energy absorption requirements increase as the square of the velocity and hence the landing speed is significant.

The procedure used to size a steel brake is given here for illustrative purposes. Similar data for carbon are not available, but scaling factors of 1.28 and 0.40 can be used to relate the steel volumes and weights, respectively, to those values for carbon [30]. Kinetic energy levels expected under the normal landing weight, maximum landing weight, and RTO conditions are first calculated using Eq. (4.5) and the appropriate aircraft weights. Brake assembly weights (W_{brake}) corresponding to each kinetic energy level are obtained from Figure 4.4 and averaged to arrive at a compromise value. The required heat sink volume (V_{brake}) is then approximated using the expression

$$V_{brake} = 3.3W_{brake} - 84.2 \tag{8.7}$$

where the constant coefficients are determined using linear regression analysis on statistical database[2].

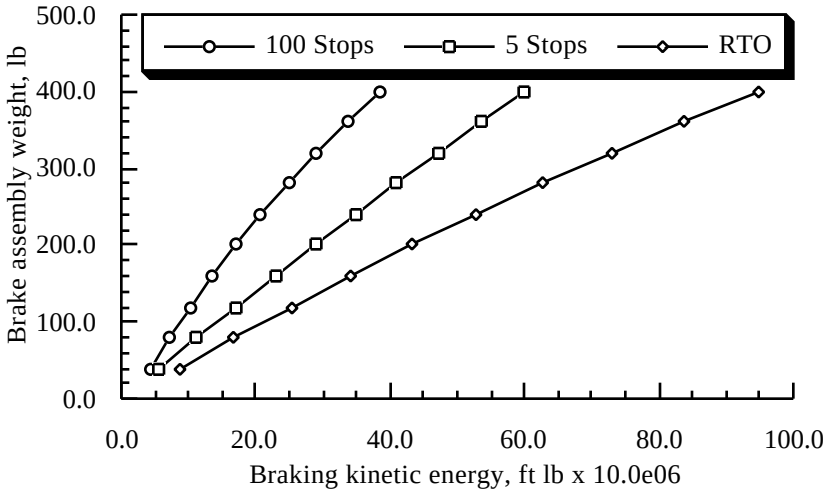

Figure 4.4 Brake assembly weight *vs.* kinetic energy level [2]

Given the tire wheel diameter as determined during the tire selection process, heat sink inner and outer diameters and the volume per inch width constant are selected from Table 4.3. Dividing the total volume by the constant then gives the necessary heat sink width. The envelope for the heat sink and torque plate carrier is established by adding 0.75 inch on the inside diameter and the end facing the wheel centerline. Finally, the piston housing envelope is approximated by adding two inches on the actuation side of the heat sink as shown in Figure 4.5 [2].

Table 4.3 Heat sink dimensions [2]

Rim dia., in	**Inner dia., in**	**Outer dia., in**	**Volume/inch width, in^2**
14.0	7.375	12.000	70.4
15.0	8.125	13.000	80.9
16.0	8.750	13.750	88.4
17.0	9.500	14.750	100.0
18.0	10.125	15.750	114.3
19.0	10.750	16.500	123.1
20.0	11.500	17.500	136.7
21.0	12.250	18.500	150.9
22.0	12.875	19.500	168.5
23.0	12.750	20.375	176.3
24.0	14.375	21.375	195.2
25.0	15.125	22.375	212.1

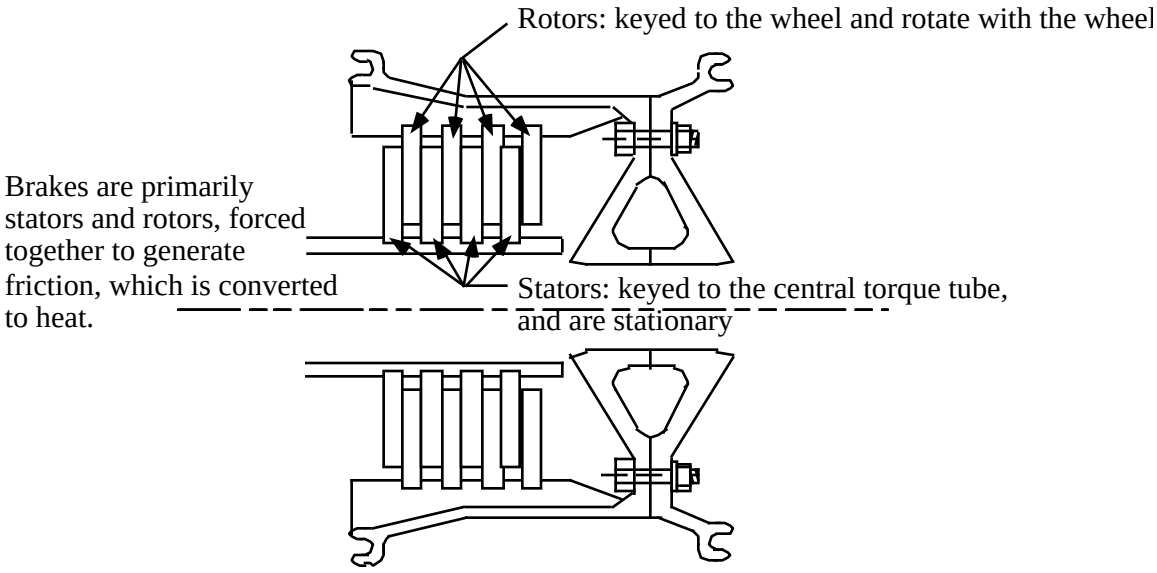

Figure 4.5 Key elements of carbon brakes. [See [2], pg 138 for more detailed view.]